Preparation, Characterization, Cytotoxicity, and Mutagenicity of a Pair of Enantiomeric Platinum(II) Complexes with the Potential To Bind Enantioselectively to DNA

Kymberley Vickery,[1a,1b] Antonio M. Bonin,[1b] Ronald R. Fenton,[1a] Shaun O'Mara,[1c] Pamela J. Russell,[1c] Lorraine K. Webster,[1d] and Trevor W. Hambley*,[1a]

School of Chemistry, University of Sydney, New South Wales, 2006, Australia, Kanematsu Laboratories, Royal Prince Alfred Hospital, Sydney, New South Wales, 2051, Australia, Toxicology Unit, National Institute of Occupational Health and Safety, G.P.O. Box 58, Sydney, New South Wales, 2001, Australia, and Peter MacCallum Cancer Institute, 481 Little Lonsdale St, Melbourne, Victoria 3000, Australia

Received May 24, 1993•

The synthesis of a pair of enantiomeric Pt(II) complexes, [Pt(*R*,*R*-eap)Cl_2] and [Pt(*S*,*S*-eap)Cl_2] (eap = *N*,*N*-diethyl-2,4-pentanediamine), designed to bind enantioselectively to GpG and ApG sequences of DNA is described. The *in vitro* cytotoxicity of each of the enantiomers toward murine leukemia and human bladder tumor cells has been measured. The *R*,*R* enantiomer was found to be more active in the leukemia cells, but the difference was not as great as expected (IC_{50}; *R*,*R* 14 μM, *S*,*S* 33 μM). In the bladder tumor cell line, no significant difference in activity was found. The two enantiomers had similar mutagenicity in the *Salmonella* reversion assay, but the *R*,*R* enantiomer was more cytotoxic in the bacterial cells. A structural analysis of the *R*,*R* enantiomer revealed that the ligand adopted an unexpected configuration, and a strain energy minimization analysis showed that this was a consequence of interactions between the diamine ligand and the dichloro ligands. The significance of the structural preferences with respect to the lower than expected enantiospecificity is discussed. Crystals of [Pt(*R*,*R*-eap)Cl_2] are monoclinic; space group, $P2_12_12_1$; a = 7.909(5), b = 12.972(9), and c = 13.269(12) Å; Z = 4; and the structure was refined to R = 0.025 (1657*F*).

Introduction

cis-DDP and related compounds are believed to effect their anticancer activity by forming bifunctional adducts with DNA, thus interfering with the replication process.[2,3] It is yet to be unequivocally established which of the bifunctional adducts is primarily responsible for the anticancer activity, and it is clearly necessary to do so before the techniques of rational drug design can be fully used to aid in the development of new Pt(II)-based anticancer drugs. The approach we have been taking has been to use molecular modeling techniques to design compounds that preferentially form a single adduct.[4-8] For instance, we have recently reported the preparation and characterization of a compound designed to bind interstrand but not intrastrand.[8] The low activity of this compound *in vitro* provides evidence that the interstrand adduct is not the adduct primarily responsible for effecting cell death and indirect evidence that the intrastrand adduct is responsible. The major intrastrand adducts are to GpG and ApG sequences.[9,10] Our modeling of these adducts has led us to the design of compounds which can act as probes to investigate the importance of the adducts in the cytotoxic process and of the factors which mediate the formation of the adducts.

Design Rationale. In our models of the GpG and ApG intrastrand adducts, and in models reported by others, the NH_3 ligands form two H bonds; one to a phosphate O atom on the 5′ side of the adduct and the other to the exocyclic oxygen of the guanine on the 3′ side.[4,5,11-13] Our studies of the reasons for the nonformation of the GpA adduct are consistent with the latter H bond being an important determinant of the binding process,[5] and others have suggested that the former H bond is also important.[14] We sought compounds which would test the hypothesis that these H bonds do mediate binding of Pt drugs to DNA. A schematic view of the *cis*-DDP/GpG adduct and the two H bonds is shown in Figure 1a. Since DNA is chiral, this adduct has a chiral sense, and it is possible to design a chiral complex which should interact enantioselectively at a GpG site. The interaction of a generalized pair of such compounds at a GpG site is shown in Figure 1b. In one case the amine H atoms have the correct dispositions to allow formation of the two H bonds, but in the other, the R groups (methyl, ethyl, or bulkier groups) are disposed toward the potential H-bonding groups. Not only would these R groups not form H bonds, but perhaps more significantly, they would produce unfavorable interactions with the DNA, particularly with the exocyclic oxygen of the 3′-guanine which we have shown to be unable to totally avoid this interaction.[5] If the enantiomer labeled 1 in Figure 1 was found to be active, and the enantiomer labeled 2 to be inactive this would provide evidence for the importance of the H bonds in mediating binding and provide indirect evidence that these adducts are responsible for the activity of *cis*-DDP and related drugs.

There have been a number of studies focusing on the different activities of the enantiomeric complexes [Pt(*R*,*R*-chxn)Cl_2] and [Pt(*S*,*S*-chxn)Cl_2][15-17] and on other enantiomeric pairs.[18] However, there have been relatively few studies where the chirality potentially resides on the N donor atoms.[19-21] The difficulty in producing and resolving such pairs of enantiomers lies in the lability of N coordinated to Pt. Under biological conditions, rapid equilibration of the stereochemistry at coordinated N would occur, resulting in no observable chiral discrimination. In order to overcome this we have used bidentate ligands in which there are also chiral centres in the C backbone of the ligand, the aim being that this nonlabile

• Abstract published in *Advance ACS Abstracts*, October 1, 1993.

0022-2623/93/1836-3663$04.00/0

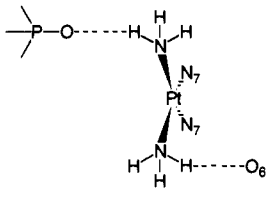

(a) Intrastrand *cis*-DDP/GpG crosslink

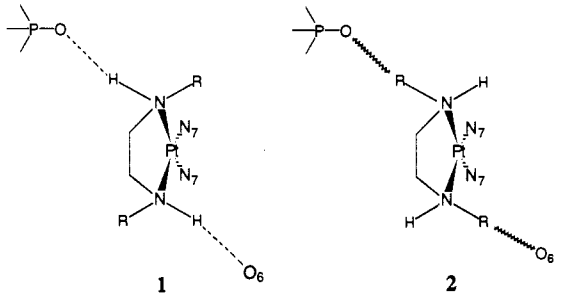

(b) Interaction between each enantiomer and DNA

Figure 1. (a) Schematic view of a intrastrand *cis*-DDP/GpG adduct. (b) Instrand interaction of two enantiomers with the GpG sequence.

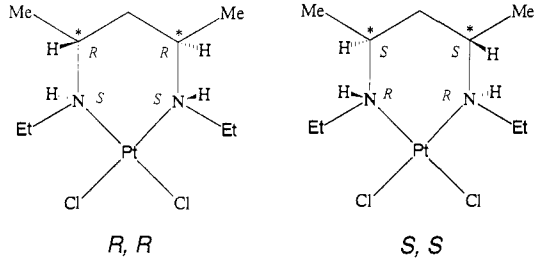

R, R *S, S*

Figure 2. Schematic views of [Pt(*R,R*-eap)Cl_2] (left) and [Pt(*S,S*-eap)Cl_2] (right).

chirality will impose the desired stereochemistry at the N atoms. Specifically, we expect that the ethyl substituents will adopt positions approximately *trans* to the methyl groups of the pentanediamine. The first pair of enantiomers we have studied that have this arrangement of chiral centers, [Pt(*R,R*-eap)Cl_2] and [Pt(*S,S*-eap)Cl_2], are shown in Figure 2. In this paper we report the preparation and chemical and biological characterization of this pair of enantiomers.

Experimental Section

Spectroscopy. ^1H and ^{13}C NMR spectra were recorded at 50.239 and 200.13 MHz, respectively, on a Bruker AC 200F spectrometer with solvents D_2O and $CDCl_3$ of 99.6% isotopic purity. Chemical shifts are reported in ppm (δ) relative to $CDCl_3$. Infrared spectra were obtained on a Perkin-Elmer 1600 series spectrophotometer using Nujol mulls on NaCl plates. Mass spectral data were recorded on a Kratos MS902 mass spectrometer. Optical rotations were measured at the sodium D line (589 nm) on a Perkin-Elmer polarimeter 241 at ambient temperatures. Solution circular dichroism spectra were measured with a JASCO J-500C spectropolarimeter and processed on a DP-500N data processor.

Preparations. *rac*- and *meso*-2,4-Pentanediamine. Acetylacetone dioxime was prepared from 2,4-pentanedione and hydroxylamine by standard methods and was reduced to 2,4-pentanediamine with Raney nickel. Separation of the racemic and *meso* isomers was carried out as described by Bosnich and Harrowfield.[22]

Resolution of *rac*-2,4-Pentanediamine. Resolution of the racemic form was by selective crystallization with (−)-dibenzoyltartaric acid and (+)-dibenzoyltartaric acid as reported by Bosnich and Harrowfield.[22] The [(*R,R*)-2,4-ptn:(−)-dibenzoyltartrate] and [(*S,S*)-2,4-ptn:(+)-dibenzoyltartrate] complexes were recrystallized to constant rotations of $[\alpha]_D = -88°$ and $+87°$, respectively (cf. literature[22] value of −91°). These were converted to the diamine dihydrochlorides which gave rotations of $[\alpha]_D = +17°$ and −16°, respectively (lit.[22] +17°).

Preparation of *meso*-*N,N'*-Diethyl-2,4-pentanediamine. The dihydrochloride salt was converted to the free base form by addition of a 5-fold excess of KOH and extraction into dichloromethane. Acetic anhydride (22.5 g, 0.22 mol) was added dropwise to the free base (5.0 g, 0.050 mol) via an air condensor with continual stirring. Dry pyridine (3 drops) was added, and the mixture was left to stand for 12 h at 5–10 °C. Excess acetic anhydride and acetic acid were removed by rotoevaporation under reduced pressure, and any remaining acetic acid was removed under high vacuum (6 h, 0.1 mmHg), leaving the product *meso*-2,4-diacetamidopentane (7.8 g, 0.045 mol, yield 10%) as a viscous yellow liquid. The diacetamide (7.0 g, 0.044 mol) was dissolved in dry tetrahydrofuran (THF) (250 mL) in a 500-mL three-necked round-bottom flask equipped with a magnetic stirrer and a reflux condensor. After slow cooling to 0 °C, freshly ground lithium aluminum hydride (15.2 g, 0.40 mol) was added carefully and with vigorous, continual stirring. After slow equilibration to room temperature, the reaction mixture was refluxed and stirred for 2 days. The suspension was then cooled to room temperature and transferred to a 1-L three-necked round-bottom flask, equipped with a magnetic stirrer. This was cooled to 0 °C, and a solution of water (36 mL) and THF (200 mL) was added cautiously with vigorous stirring. Solids were filtered off, and the filter-cake was extracted three times with boiling THF. The combined THF filtrate and washings were evaporated under reduced pressure to give meso-*N,N'*-diethyl-2,4-pentanediamine (4.9 g, yield 72%). The resultant diamine was stored under nitrogen.

Preparation of *rac*-*N,N'*-Diethyl-2,4-pentanediamine. The (*R,R*)-(−) and (*S,S*)-(+) enantiomers of 2,4-pentanediamine were converted to the free base and ethylated by the procedures outlined above for the *meso* isomer. Average yield based on the free base form was 35%: mass spectra found, M^+ 158, $C_9H_{22}N_2$ requires 158.29; ^1H NMR ($CDCl_3$) δ 1.1 (t and s), 1.45 (dd), 2.6–2.7 (quartet and sextet); ^{13}C NMR ($CDCl_3$) δ 16, 21, 41, 44, 51.

Dichloro-*meso*-(*N,N'*-diethyl-2,4-pentanediamine)platinum(II). The procedures outlined by Dhara[23] and by Rochon and Kong[24] were adapted as follows in the preparation of the Pt(II) complexes. An aqueous solution of $K_2[PtCl_4]$ (0.415 g, 1.00 mmol, Aldrich) in water (3 mL) was mixed with KI (4.0 g, 0.024 mol) and stirred for 15 min. The formation of $K_2[PtI_4]$ was indicated by the formation of a dark black yellow color. To this solution was added an equimolar amount of *meso*-*N,N'*-diethyl-2,4-pentanediamine (0.607 g, 1.00 mmol) in water (1 mL), and a dark olive colored precipitate formed almost immediately. The mixture was left to stir for 24 h, and the [Pt(*meso*-eap)I_2] complex was filtered, washed with cold water, and allowed to dry for 24 h over silica gel. To the complex (0.821 mmol, 82% yield), $AgNO_3$ (0.0279 g, 0.164 mmol) in water (2 mL) was added, and the mixture was then stirred for 2 days. The resultant AgI precipitate was removed by filtration and washed with cold water, a further 2–3 drops of NaCl (0.5 M) was added to the filtrate to remove any excess silver ions. The procedure was repeated until there was no immediate precipitate after the addition of one drop of NaCl solution. The volume of the filtrate was then reduced to 4 mL by rotoevaporation, and a 25-fold excess of solid NaCl (0.021 g, 0.36 mmol) was added. After stirring (10 min), a pale yellow precipitate formed which was filtered and washed thoroughly with cold water to remove excess water-soluble salts. The product *cis*-[Pt(*meso*-eap)Cl_2], was dried in a dessicator for 12 h (0.148 g, yield 70% with respect to the ligand).

Dichloro-(*R,R*)- and -(*S,S*)-(*N,N'*-diethyl-2,4-pentanediamine)platinum(II). Both enantiomers were synthesized from the resolved diamine by a method analogous to that described for the *meso* isomer. The average yield based on the ligand was 50%.

Cytotoxicity Assays. The recently established human bladder cancer cell line used was UCRU BL13/0[25] which was grown as a monolayer in RPMI 1640 culture media supplemented with

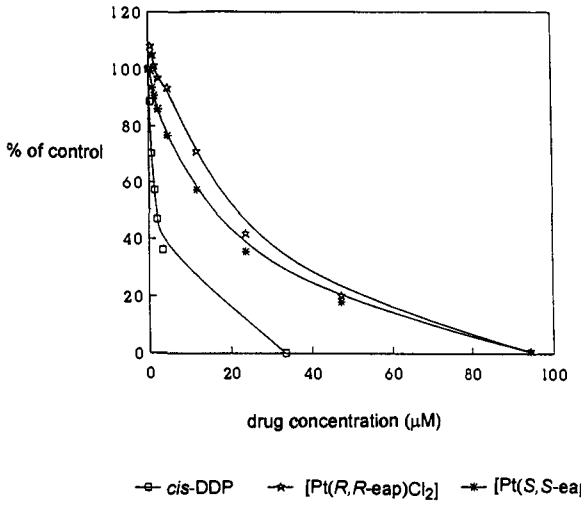

Figure 3. Dose–response of human bladder cancer cell line UCRU BL13/0 to *cis*-DDP, [Pt(*R*,*R*-eap)Cl_2], and [Pt(*S*,*S*-eap)Cl_2].

Table I. Cytotoxicity (IC_{50}) Values (μM) Determined in Human Bladder Tumor and Murine Leukemia Cell Lines

cell line	[Pt(*R*,*R*-eap)Cl_2]	[Pt(*S*,*S*-eap)Cl_2]	*cis*-DDP
human bladder	22	18	4
murine leukemia	14	33	0.6

10% foetal calf serum (FCS), penicillin (50 ic units/mL), and streptomycin (50 μg/mL) and maintained in a humidified incubator at 37 °C in 7.5% CO_2, 5% O_2, and 87.5% N_2. Cells were maintained in exponential growth phase by subculturing routinely with trypsin–EDTA. IC_{50} values in the drug assays were determined using log-phase cultures grown in microtitre plates. [Pt(*R*,*R*-eap)Cl_2], [Pt(*S*,*S*-eap)Cl_2], and *cis*-DDP stock solutions were made up fresh in RPMI 1640 medium at concentrations of 2 mg/mL. Cells were exposed to the drug at a range of concentrations (0–95 μM) for a period of 4 days in tissue culture. In each drug assay, *cis*-DDP was used as a standard. Cell viability following treatment was determined using the MTT (3-[4,5-dimethylthiazol-2-yl]-2,5-diphenyl bromide; thiazolyl blue) cytotoxicity assay.[26] The variation in cytotoxicity with drug concentration for the two enantiomers and for *cis*-DDP are displayed in Figure 3, and IC_{50} values are listed in Table I.

L1210 mouse leukemia cells were grown as suspension cultures in MEM (minimum essential medium, Eagle's) plus 1% glutamine and 10% FCS (Flow Laboratories). [Pt(*R*,*R*-eap)Cl_2] and [Pt(*S*,*S*-eap)Cl_2] were dissolved in dimethyl sulfoxide (DMSO), and the mixture was then immediately added to the medium at several concentrations over a 2-log range with a final DMSO concentration in the medium of 0.5%. *cis*-DDP was dissolved in saline. Growth inhibition was tested by incubation of log-phase cells at 37 °C in a humidified incubator gassed with 10% CO_2/90% air for 48 h in the presence of the drug. Cells were then counted using a Coulter counter, and the IC_{50} (μM), or concentration causing 50% inhibition of cell growth, was determined from the curve of percentage growth versus dose. Control cultures exposed only to the vehicle were included with each test and were used to represent 100% growth. The results given in Table I are the mean of at least two determinations.

Mutagenicity Assays with Bacteria. *Salmonella typhimurium* stains TA100, TA97a, TA102, TA98, and TA1535 were obtained from Provessor B. N. Ames, University of California, Berkeley, CA, and cultured as described.[27] Fresh broth cultures of each strain were incubated at 37 °C in a shaking water bath for 10 h prior to each assay. Top agar, supplemented with a trace of histidine and biotin, was dispensed in 2-mL volumes into 5-mL plastic vials in a 45 °C water bath. Broth culture and the test chemical (0.1 mL of each dissolved in freshly prepared DMSO solution) were then added to each vial. Duplicate plates at each dose level were incubated at 37 °C for 48 h before counting revertant colonies with an Artek Model 880 counter. Mutagenicities for TA100 and TA97a are recorded in Tables II and III, respectively.

Table II. Mutagenicity of [Pt(*R*,*R*-eap)Cl_2] and [Pt(*S*,*S*-eap)Cl_2] and *cis*-DDP in *S. typhimurium* TA100

	revertants/plate		
dose (μg/plate)	[Pt(*R*,*R*-eap)Cl_2]	[Pt(*S*,*S*-eap)Cl_2]	*cis*-DDP
0	125, 138	125, 138	125, 138
1			451, 470
2.5	172, 174	132. 127	726, 713
5	161, 169	157. 158	892, 823
10	220, 219	171. 174	629, 715
12.5	toxic	162, 172	toxic
25		241, 234	
30		290, 300	
40		302, 295	
50		360, 388	
60		389, 391	
250		861, 900	

Table III. Mutagenicity of [Pt(*R*,*R*-eap)Cl_2] and [Pt(*S*,*S*-eap)Cl_2] and *cis*-DDP in *S. typhimurium* TA97a

	revertants/plate	
dose (μg/plate)	[Pt(*R*,*R*-eap)Cl_2]	[Pt(*S*,*S*-eap)Cl_2]
0	160, 165	160, 165
5	238, 247	
10	276, 283	229, 245
20	toxic	306, 297
30		385, 425
40		410, 433
50		510, 471

Table IV. Crystal Data for [Pt(*R*,*R*-eap)Cl_2]

crystal system	orthorhombic
space group	$P2_12_12_1$
a, Å	7.909(5)
b, Å	12.972(9)
c, Å	13.269(12)
V, Å^3	1361.4(18)
formula weight	424.28
D_{calcd}, g cm^{-3}	2.070
empirical formula	$C_9H_{22}Cl_2N_2Pt$
Z	4
absorp coeff, cm^{-1}	107.46
trans coeffs	0.356–0.105
temperature, °C	21
λ, Å	0.71069
R (F_o)	0.025
R_w	0.027

Crystallography. Cell constants were determined by least-squares fits to the setting parameters of 25 independent reflections, measured and refined on an Enraf-Nonius CAD4-F diffractometer with a graphite monochromator. The crystallographic data are summarized in Table IV. Data were reduced and Lorentz, polarization, and absorption corrections were applied using the Enraf-Nonius structure determination package (SDP).[28] The structure was solved by heavy-atom methods using SHELX-76[29] and was refined by full-matrix least-squares analysis with SHELX-76. Hydrogen atoms were included at calculated sites (C–H, N–H 0.97 Å) with individual isotropic thermal parameters. All other atoms except minor contributors to disordered groups were refined anisotropically. The absolute configuration was confirmed by inverting all coordinates and refining; at convergence the *R* value for the alternative configuration was 0.037. Scattering factors and anomalous dispersion corrections for Pt were taken from ref 30, and for all others the values supplied in SHELX-76 were used. The atomic nomenclature is defined in Figure 4.[31] Listings of non-hydrogen atom coordinates, bond lengths and angles, H atom coordinates, anisotropic thermal parameters, close intermolecular contacts, torsion angles, and observed and calculated structure factor amplitudes are available as supplementary material.

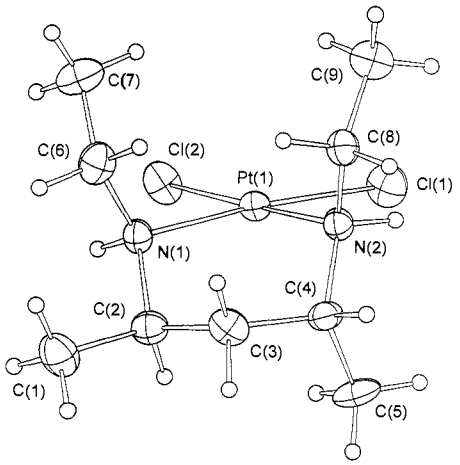

Figure 4. ORTEP plot of [Pt(*R*,*R*-eap)Cl_2] giving the crystallographic atom numbering. The configuration at N(1) is *R* and at N(2) is *S*; 30% probability ellipsoids are shown.

Table V. Strain Energies of the Conformers and Configurations of [Pt(*R*,*R*-eap)Cl_2] and [Pt(*S*,*S*-eap)Cl_2]

conformer	[Pt(*R*,*R*-eap)Cl_2]	[Pt(*S*,*S*-eap)Cl_2]	strain energy, kJ mol^{-1}
chair	{*RR*, *RR*}	{*SS*, *SS*}	53.3
	{*RR*, *RS*}	{*SS*, *SR*}	52.2
	{*RR*, *SR*}	{*SS*, *RS*}	83.4
	{*RR*, *SS*}	{*SS*, *RR*}	63.1
skew-boat	{*RR*, *RR*}	{*SS*, *SS*}	61.8
	{*RR*, *RS*}	{*SS*, *SR*}	63.3
	{*RR*, *SS*}	{*SS*, *RR*}	91.8

Molecular Modeling. All diastereomers of [Pt(*R*,*R*-eap)Cl_2] were subjected to strain energy minimization analysis using a force field described previously.[32] Starting models were generated using the HyperChem system[33] implemented on a 486-DX computer system, and strain energy minimization was performed using MOMECPC,[34] a modified version of MOMEC-87,[35] also running on the 486-DX computer. Final strain energies are listed in Table V. Configurations are indicated by listing the chirality at each of the C atoms first followed by the chirality at each of the N atoms.

Results and Discussion

Ligand Synthesis. The aim was to produce an enantiomeric pair of N,N′-diethylated diamines. Resolution of the chiral diamine was carried out prior to ethylation as procedures for this were already well established. Next, a synthetic route which gave a product with exactly one ethyl substituent on each nitrogen atom was essential. Reactions of diamines with alkylating compounds such as alkyl halides produce a mixture of monoalkylated, N,N-dialkylated, trialkylated, and tetralkylated products in addition to the desired N,N′-dialkylated compound. Extensive purification procedures, if at all possible, are required to produce this desired product with an acceptable purity for biological testing. Therefore, we developed a facile route to produce a N,N′-disubstituted 2,4-pentanediamine. This involved formation of a diacetamide from the parent diamine followed by the reduction of the amide groups to secondary amine groups. This method gave the desired products in high purity and with an acceptable yield.

Description of the Structure. The structure consists of neutral [Pt(*R*,*R*-eap)Cl_2] molecules with only very weak H bonds between the H(amine) atoms of one molecule and the chloro ligands of a symmetry-related molecule. There are closer intramolecular contacts between the H(amine) atoms and the chloro ligands, though whether these should be described as H bonds is debatable since such contacts are inevitable in this configuration of the complex. The configuration of the ligand is not that which was anticipated; *viz* a configuration with the ethyl substituents *trans* to the methyl groups of the pentane moiety and therefore *trans* to each other. Rather, the configuration adopted has the ethyl groups disposed on the same side of the Pt atom. The ethyl group nearest C(5) is *trans* to this methyl group but that nearest C(1) is *cis* to that methyl group. The reasons for the occurrence of this unexpected configuration are discussed below. The chirality at N(1) is *R* and that at N(2) is *S*, and the overall configuration then is *RR*, *RS*. The conformation of the six-membered chelate ring is a chair; a least-squares plane through the four atoms defining the seat [N(1), N(2), C(2), and C(4)] reveals no deviations greater than 0.003 Å. Pt(1) and C(3) lie 1.058 and 0.654 Å, respectively, on opposite sides of this plane. One of the methyl groups [C(1)] of the pentane moiety is equatorial with respect to the chair and the other [C(5)] is axially disposed, as are both ethyl substituents.

Molecular Modeling. The six-membered chelate ring in [Pt(*R*,*R*-eap)Cl_2] (and in [Pt(*S*,*S*-eap)Cl_2]) can adopt a chair or a skew-boat conformation, and both possibilities were subjected to strain energy minimization analysis. *R* and *S* chiralities are possible at each N atom which leads to four sets of configurations at the atoms (*R*,*R*; *R*,*S*; *S*,*R*; *S*,*S*) for the chair conformer of [Pt(*R*,*R*-eap)Cl_2] but only three for the skew-boat conformer (*R*,*R*; *S*,*R*; *S*,*S*) since the 2-fold symmetry of the skew-boat leads to the equivalence of the *R*,*S* and *S*,*R* configurations. There are a similar number of configurations for [Pt(*S*,*S*-eap)Cl_2], and in order to distinguish the various combinations we have used the notation {*RR*, *SR*} for example, where the first pair of chiralities are those at the C atoms and the second pair are those at the N atoms. Calculations were only performed on the configurations and conformations of [Pt(*R*,*R*-eap)Cl_2], but the energies for those of [Pt(*S*,*S*-eap)Cl_2] will be the same except the chiralities at the N atoms are inverted.

The strain energies of the configurations skew-boat conformer are uniformly higher than those of the chair (Table V) so discussion hereafter is limited to configurations of the latter. Two configurations, {*RR*, *RS*} and {*RR*, *RR*}, have similar energies, and these are substantially (>10 kJ mol^{-1}) greater than those of the other configurations. The {*RR*, *RR*} configuration was the one we anticipated would be most stable because it has the ethyl substituents *trans* to the methyl groups of the ligand. However, the stability of the {*RR*, *RS*} configuration was not originally anticipated, though it is the configuration observed in the crystal structure. The reason this apparently unfavorable arrangement is adopted is related to the interactions between the diamine ligand and the chloro ligands. The {*RR*, *RS*} configuration is the only one in which both H(amine) atoms lie in or close to the coordination plane. Other arrangements have one or more of the ethyl substituents adjacent to the chloro ligands resulting in repulsive Cl···H interactions where, in the {*RR*, *RS*} configuration Cl···H(amine) interactions, that are at least electrostatically favorable, are found. Bosnich and Sullivan[36] have reported that the energy differences between different stereoisomers are influenced by other groups coordinated to the Pt atom.

The basis of our hypothesis that [Pt(*R,R*-eap)Cl_2] would bind more readily to DNA than would [Pt(*S,S*-eap)Cl_2] was that it would largely adopt the {*RR, RR*} configuration and [Pt(*S,S*-eap)Cl_2] the {*SS, SS*} configuration. However, the availability of a low-energy configuration with different chiralities at N means that less than complete enantioselectivity must be anticipated.

Cytotoxicity Studies. Both enantiomers of [Pt(*rac*-eap)Cl_2] show significant cytotoxicity in L1210 murine leukemia cells and human bladder tumor cells. In the murine cells, the *R,R* is marginally more active than the *S,S* enantiomer which is contrary in both direction and magnitude to what was anticipated. In the bladder tumor cell line, no significant difference in activities was found for the two enantiomers. Possible reasons for these unexpected results are discussed below. Both complexes are substantially less active than *cis*-DDP.

Mutagenicity Studies. The two enantiomers of [Pt(*rac*-eap)Cl_2] were tested for their mutagenicity toward *S. typhimurium* strains TA97a, TA98, TA100, TA102, and TA1535. No significant activity was detected at up to 60 μg per plate for [Pt(*S,S*-eap)Cl_2] and 10 μg per plate for [Pt(*R,R*-eap)Cl_2] with strains TA98, TA102, and TA1535. Significant activity was observed against strains TA97a and TA100 and these results are given in Tables II and III. All compounds gave linear or near-linear dose–response curves between 2.5 and 10 μg/plate. At concentrations above 10 μg/plate, [Pt(*R,R*-eap)Cl_2] was cytotoxic, and this hampered the reliable determination of the mutagenicity of this enantiomer. Interestingly, the *R,R* showed much greater cytoxicity than the *S,S* enantiomer in this system. The two enantiomers had similar, but not significant, mutagenicities at concentrations below 10 μg/plate. [Pt(*S,S*-eap)Cl_2] caused a doubling in revertant colonies at 30 μg/plate in TA100 and at 20 μg/plate in TA97a. *cis*-DDP, by comparison, showed a highly mutagentic response (330 revertants above background) at 1 μg/plate in TA100. This is more mutagenic than was reported by Benedict *et al.* where 200 revertants were induced at the same concentration.[37] TA97a was found to be more sensitive to both enantiomers than was TA100. TA100 reversions are caused by base-pair substitutions, and TA97a is sensitive to frame shifts.

Conclusions

The aim of this study was to develop and prepare an enantiomeric pair of Pt(II) complexes that would show highly enantioselective interactions with DNA and therefore, by inference, enantiospecific cytotoxicity. The synthesis of a resolved pair of N,N′-dialkylated enantiomeric ligands was achieved as was the synthesis of their dichloroplatinum(II) complexes. The *R,R* enantiomer had a higher *in vitro* cytotoxicity in L1210 cells, but this difference was not as large as expected on the basis of our working hypothesis. A crystal structure analysis of the *R,R* enantiomer revealed that the ligand did not adopt the arrangement that was originally expected. Strain energy minimization analysis of the possible configurations is consistent with the observation of that seen in the crystal structure and showed that its relative stability is due to interactions between the amine ligand and the chloro ligands. A consequence of the availability of more than one configuration is that the complex, [Pt(*rac*-eap)Cl_2], does not meet the design criteria of having the H(amine) atoms rigorously disposed on opposite sides of the coordination plane and this in turn may explain the lower than expected enantioselectivity in its action. Curiously, the enantiomers have similar mutagenicities, but the *R,R* is substantially more cytotoxic toward bacterial cells than is the *S,S* enantiomer. These data confirm the observations of Kidani and co-workers that chiral Pt(II) complexes behave enantioselectively in their interactions with their biological targets. In order to test our hypothesis that higher enantioselectivity can be achieved by having chiral N atoms, we are currently persuing the preparation of ligands that more rigorously impose the desired chirality.

Acknowledgment. The support of the Sydney University Cancer Research Fund and the Australian Research Council is gratefully acknowledged. We wish to thank Mrs. Bernadette Linahan for assistance with the cytotoxicity assays. The views expressed in this article are those of the authors and do not necessarily reflect those of the National Occupational Health and Safety Commision.

Supplementary Material Available: Tables of crystal data, positional and thermal parameters, bond lengths and angles, torsion angles, least-squares planes, and nonbonded distances (8 pages); observed and calculated structure factors (10 pages). Ordering information is given on any current masthead page.

References

(1) (a) School of Chemistry, University of Sydney. (b) Nation Institute of Occupational Health and Safety. (c) Kanematsu Laboratories, Royal Prince Alfred Hospital. (d) Peter MacCallum Cancer Institute.
(2) Pinto, A. L.; Lippard, S. J. Binding of the antitumor drug *cis*-diamminedichloroplatinum(II) (cisplatin) to DNA. *Biochem. Biophys. Acta* **1985**, *780*, 167–180.
(3) Sheibani, N.; Jennerwein, M. M.; Eastman, A. DNA repair in cells sensitive and resistant to *cis*-diamminedichloroplatinum(II): Host cell reactivation of damaged plasmid DNA. *Biochemistry* **1989**, *28*, 3120–3124.
(4) Hambley, T. W. Why does cisplatin bind to ApG but not GpA sequences of DNA? A molecular mechanics analysis. *J. Chem. Soc., Chem. Commun.* **1988**, 221–223.
(5) Hambley, T. W. A molecular mechanics analysis of the stereochemical factors influencing monofunctional and bifunctional binding of *cis*-diamminedichloroplatinum(II) to adenine and guanine nucleobases in the sequences d(GpApGpG):d(CpCpTpC) and d(GpGpApG):d(CpTpCpC) of A- and B-DNA. *Inorg. Chem.* **1991**, *30*, 937–942.
(6) Hambley, T. W. What can be learnt from computer generated models of interactions between DNA and Pt(II) based anti-cancer drugs? *Comm. Inorg. Chem.* **1992**, *14*, 1–26.
(7) Ling, E. C. H.; Allen, G. W.; Hambley, T. W. The preparation and characterisation of some aminesulfoxideplatinum(II) complexes. *J. Chem. Soc., Dalton Trans.*, in press.
(8) Ling, E. C. H.; Allen, G. W.; Hambley, T. W. The DNA binding of platinum(II) complex designed to bind interstrand but not intrastrand. Manuscript in preparation.
(9) Eastman, A. Characterization of the adducts produced in DNA by *cis*-diamminedichloroplatinum(II) and *cis*-dichloro-(ethylenediamine)platinum(II). *Biochemistry* **1983**, *22*, 3927–3933.
(10) Fichtinger-Schepman, A. M. J.; van der Veer, J. L.; den Hartog, J. H. J.; Lohman, P. H. M.; Reedijk, J. Adducts of the anti-tumor drug *cis*-diamminedichloroplatinum(II) with DNA: formation, identification and quantitation. *Biochemistry* **1985**, *24*, 707–713.
(11) Kozelka, J.; Pestko, G. A.; Lippard, S. J.; Quigley, G. J. Molecular mechanics calculations on *cis*-[$Pt(NH_3)_2$[dGpG]] adducts in two oligonucleotide duplexes. *J. Am. Chem. Soc.* **1985**, *107*, 4079–4081.
(12) Kozelka, J.; Pestko, G. A; Quigley, G. J.; Lippard, S. J. High-salt and low-salt models for kinked adducts of *cis*-diamminedichloroplatinum(II) with oligonucleotide duplexes. *Inorg. Chem.* **1986**, *25*, 1075–1077.
(13) Kozelka, J.; Archer, S.; Pestko, G. A.; Lippard, S. J.; Quigley, G. J. Molecular mechanics modeling of oligonucleotide adducts of the antitumor drug *cis*-diamminedichloroplatinum(II). *Biopolymers* **1987**, *26*, 1245–1271.
(14) Reedijk, J. The relevance of hydrogen bonding in the mechanism of action of platinum antitumor compounds. *Inorg. Chim. Acta* **1992**, *198–200*, 873–881.
(15) Kidani, Y.; Inagaki, K.; Iigo, M.; Hoshi, A.; Kuretani, K. Antitumor activity of 1,2-diaminocyclohexane-platinum complexes against sarcoma-180 ascites form. *J. Med. Chem.* **1978**, *21*, 1315–1318.
(16) Kidani, Y.; Noji, M.; Tashior, T. Antitumor activity of platinum(II) complexes of 1,2-diaminocyclohexane isomers. *Gann.* **1980**, *71*, 637–643.

(17) Noji, M.; Okamato, K.; Kidani, Y.; Tashiro, T. Relation of conformation to antitumor activity of platinum(II) complexes of 1,2-cyclohexanediamine and 2-(aminomethyl)cyclohexylamine isomers against leukemia P388. *J. Med. Chem.* **1981**, *24*, 508–515.
(18) Noji, M.; Motoyama, S.; Tashiro, T.; Kidani, Y. Synthesis and antitumor activity of Pt(II) complexes containing 2,3-diaminopropanol isomers. *Chem. Pharm. Bull.* **1983**, *31*, 1469–1473.
(19) Saito, R.; Goto, M.; Hirose, J.; Kidani, Y. Diastereoisomers of platinum(II) complexes with chiral *N*-substituted 1,2-diamines. I. Structure and isomerization of dichloro{(*R*)-2-[(2-methyl-2-aminopropyl)amino]-1-butanol}platinum(II). *Bull. Chem. Soc. Jpn.* **1992**, *65*, 1428–1437.
(20) Saito, R.; Goto, M.; Hirose, J.; Kidani, Y. Diastereoisomers of platinum(II) complexes with chiral *N*-substituted 1,2-diamines. II. Structures of dichloro[(*S*)-1-(2-amino-2-methylpropyl)amino-1-propanol}platinum(II). *Bull. Chem. Soc. Jpn.* **1992**, *65*, 2118–2126.
(21) Xu, Y.; Natile, G.; Intini, F. P.; Marzilli, L. G. Stereochemically controlled ligands influence atropisomerization of Pt(II) nucleotide complexes. Evidence for head-to-head and stable Λ head-to-tail atropisomers. *J. Am. Chem. Soc.* **1990**, *112*, 8177–8179.
(22) Bosnich, B.; Harrowfield, J. MacB. A regional rule for the optical activity of conformational isomers of octahedral transition metal complexes. *J. Am. Chem. Soc.* **1972**, *94*, 3425–3438.
(23) Dhara, S. C. A rapid method for the synthesis of *cis*-$[Pt(NH_3)_2Cl_2]$. *Indian J. Chem.* **1970**, *8*, 193–194.
(24) Rochon, F. D.; Kong, P. C. Iodo-bridged complexes of platinum(II) and synthesis of *cis* mixed-amine platinum(II) compounds. *Can. J. Chem.* **1986**, *64*, 1894.
(25) Russell, P. J.; Wass, J.; Lukeis, R.; Garson, M.; Jelbart, M.; Wills, E.; Phillips, J.; Brown, J.; Carrington, N.; Vincent, P.; Raghavan, D. Characterization of cell lines derived from a multply aneuploid human bladder transitional-cell carcinoma UCRU-BL-13. *Int. J. Cancer* **1989**, *44*, 276–285.
(26) Mosmann, T. Rapid colorimetric assay for cellular growth and survival. Application to proliferation and cytotoxicity assays. *Immunol. Methods* **1983**, *65*, 55–64.
(27) Bonin, A. M.; Rosario, C. A.; Duke, C. C.; Baker, R. S. U.; Ryan, A. J.; Holder, G. M. The mutagenicity of dibenz(a,j)acridine, some metabolites and other derivatives in bacteria and mammalian cells. *Carcinogenesis* **1989**, *10*, 1079–1084.
(28) Enraf-Nonius Structure Determination Package, Enraf-Nonius, Delft, Holland, 1985.
(29) Sheldrick, G. M. *SHELX-76, A Program for X-Ray Crystal Structure Determination*; Univ. of Cambridge: England, 1976.
(30) Cromer, D. T.; Waber, J. T. *International Tables for X-Ray Crystallography*; Kynoch Press: Birmingham, England, 1974; Vol. IV.
(31) Figures were drawn with ORTEP (Johnson, C. K. *ORTEP, A Thermal Ellipsoid Plotting Program*; Oak Ridge National Labs.: Oak Ridge, TN, 1965).
(32) Hambley, T. W. The influence of inter-ligand interactions on isomer stabilities and barriers to isomer interconversion in di(ammine)- and di(amine)bis(purine)platinum(II) complexes. A molecular mechanics study. *Inorg. Chem.* **1988**, *27*, 1073–1077.
(33) HyperChem, Release 2 for Windows, Autodesk, Sausalito, CA.
(34) Hambley, T. W.; Comba, P. C. Unpublished results.
(35) Hambley, T. W. *MOMEC-87, Program for Strain Energy Minimisation*; Univ. of Sydney: Sydney, 1987.
(36) Bosnich, B.; Sullivan, E. A. Conformational dissymmetry. Axial-equatorial isomer distributions of *N*-methyl substituted aliphatic five-membered chelate rings. *Inorg. Chem.* **1975**, *14*, 2768–2773.
(37) Benedict, W. F.; Baker, M. S.; Haroun, L.; Choi, E.; Ames, B. N. Mutagenicity of cancer chemotherapeutic agents in the *salmonella*-microsome test. *Cancer Res.* **1977**, *37*, 2209–2213.